

University of Montana

ScholarWorks at University of Montana

Graduate Student Theses, Dissertations, &
Professional Papers

Graduate School

1985

Temporal Integration of Auditory Signals for Various Binaural Phase Conditions.

Ruth A. Fugleberg
The University of Montana

Follow this and additional works at: <https://scholarworks.umt.edu/etd>

Let us know how access to this document benefits you.

Recommended Citation

Fugleberg, Ruth A., "Temporal Integration of Auditory Signals for Various Binaural Phase Conditions." (1985). *Graduate Student Theses, Dissertations, & Professional Papers*. 9307.
<https://scholarworks.umt.edu/etd/9307>

This Thesis is brought to you for free and open access by the Graduate School at ScholarWorks at University of Montana. It has been accepted for inclusion in Graduate Student Theses, Dissertations, & Professional Papers by an authorized administrator of ScholarWorks at University of Montana. For more information, please contact scholarworks@mso.umt.edu.

COPYRIGHT ACT OF 1976

THIS IS AN UNPUBLISHED MANUSCRIPT IN WHICH COPYRIGHT SUBSISTS. ANY FURTHER REPRINTING OF ITS CONTENTS MUST BE APPROVED BY THE AUTHOR.

MANSFIELD LIBRARY
UNIVERSITY OF MONTANA

DATE: 1985

**Temporal Integration of Auditory Signals for
Various Binaural Phase Conditions**

Ruth A. Fugleberg

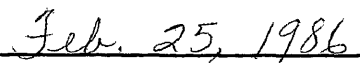
BA, University of Montana, 1983

Professional paper submitted in partial
fulfillment of the requirements for the degree of
Master of Communication Science and Disorders
University of Montana
December, 1985

Approved by:


Chairman, Board of Examiners


Dean, Graduate School


Date

UMI Number: EP72618

All rights reserved

INFORMATION TO ALL USERS

The quality of this reproduction is dependent upon the quality of the copy submitted.

In the unlikely event that the author did not send a complete manuscript and there are missing pages, these will be noted. Also, if material had to be removed, a note will indicate the deletion.



UMI EP72618

Published by ProQuest LLC (2015). Copyright in the Dissertation held by the Author.

Microform Edition © ProQuest LLC.

All rights reserved. This work is protected against
unauthorized copying under Title 17, United States Code



ProQuest LLC.
789 East Eisenhower Parkway
P.O. Box 1346
Ann Arbor, MI 48106 - 1346

ABSTRACT

The effect of signal duration on various binaural phase conditions, is currently a controversial topic in psychoacoustics, especially for durations less than 20 ms. The present study utilized the masking-level difference paradigm (S_0N_0 , $S_\pi N_0$, and S_0N_π) to investigate the temporal integration of energy for 2- to 100-ms, 500-Hz tones in 30.7 dB pressure-spectrum level, continuous broadband noise. The data from the two subjects suggested that the signal durations at which the measured thresholds increased by more than predicted by perfect power summation were different among the S_0N_0 , $S_\pi N_0$, and S_0N_π conditions. In general, the masking-level differences, reflecting the differential temporal integration for the three conditions, were largest for 6- to 10-ms signals, and were smallest at the extremes of the signal duration continuum. Estimates of the critical bandwidths for S_0N_0 , $S_\pi N_0$, and S_0N_π suggest that different critical bandwidths may exist for the three listening conditions.

ACKNOWLEDGEMENTS

I would like to express my sincere thanks to Dr. Richard H. Wilson for offering me the opportunity to do this research, for his invaluable assistance throughout the project, and for his patience in answering my many questions. I also would like to thank Kim Webb for the many hours she spent as a subject for the experiment, and my parents, Paul and Mary Lou Fugleberg, for their never-ending love and support.

TABLE OF CONTENTS

Abstract.	ii
Acknowledgements.	iii
List of Figures	v
List of Tables.	vi
Introduction.	1
Terminology	1
Temporal Integration.	3
Critical Bands.	12
Temporal Integration and Critical Bands	13
Methods	21
Results	28
Discussion.	33
References.	42

LIST OF FIGURES

Figure 1. The relation between the masked thresholds (in dB SPL) and signal duration (in ms) for 400-Hz, 670-Hz, 1000-Hz and 1900-Hz pure tones. (From Garner & Miller, 1947.)	4
Figure 2. The relation between absolute threshold (in dB SPL) and signal duration (in ms) for broadband noise, a 1000-Hz pure tone, and a filtered 1000-Hz pure tone with a 100-Hz bandwidth. (From Garner, 1947.)	5
Figure 3. The relation between absolute threshold (in dB SPL) and signal duration (in ms) for 250-Hz, and 4000-Hz pure tones. (From Garner, 1947.)	7
Figure 4. The average minimum audible sound-pressure level curve for a TDH-39 earphone. (From American National Standards Institute, 1969.)	11
Figure 5. The relation between masked thresholds (in dB SPL) and the 500-Hz signal duration (in ms) for S_0N_0 and $S_{\pi}N_0$. (From Blodgett, Jeffress & Taylor, 1958.)	17
Figure 6. The relation between masked thresholds (in dB SPL) and the 500-Hz signal duration (in ms) for S_0N_0 and $S_{\pi}N_0$. (From Wilson & Fowler, 1985.)	18
Figure 7. The mean masking-level differences (in dB) obtained for four 500-Hz signal durations (in ms). (From Wilson & Fowler, 1985.)	20
Figure 8a. The acoustic power spectrum of the 2-ms, 500-Hz signal determined from 32 samples of the signal on a NBS-9A coupler and a spectrum analyzer (Bruel & Kjaer, Type 2033).	24
Figure 8b. The acoustic power spectra of the 4- through 20 ms, 500-Hz signals determined from 32 samples of each signal on a NBS-9A coupler and a spectrum analyzer (Bruel & Kjaer, Type 2033).	25
Figure 9. The acoustic power spectra of the 25- through 100 ms, 500-Hz signals determined from 32 samples of each signal on a NBS-9A coupler and a spectrum analyzer (Bruel & Kjaer, Type 2033).	26
Figure 10. The individual and mean 500-Hz thresholds (in dB SPL) for S_0N_0 , $S_{\pi}N_0$, and S_0N_{π} obtained for the 13 durations (in ms) in 30.7-dB pressure-spectrum level, broadband noise.	30
Figure 11. The individual and mean $S_{\pi}N_0$ and S_0N_{π} 500-Hz masking-level differences (in dB) obtained for the thirteen durations (in ms) in 30.7-dB pressure-spectrum level, broadband noise.	31

Figure 12. The individual thresholds (in dB), corrected for perfect power summation as a function of the 500-Hz signal duration for S_0N_0 , $S_{\pi}N_0$, and S_0N_{π} conditions.	34
Figure 13. The relation between predicted and measured thresholds in dB SPL for 500-Hz pure tones.	36
Figure 14. A comparison of the 500-Hz $S_{\pi}N_0$ masking-level differences reported by the present study, Blodgett et. al, (1958), and Wilson and Fowler (1985).	38

LIST OF TABLES

Table 1. The relations between signal duration, bandwidth and perfect power summation	9
Table 2. The relationship between critical bandwidth and center frequency. (From Scharf, 1970.)	14
Table 3. The half-power points or the 3-dB down points of the respective spectrum of the 13 signal durations. The 3-dB bandwidth also is listed.	27
Table 4. The thresholds and masking-level differences (MLD) obtained from six trials for each of the 13 signal durations in 68-dB SPL broadband noise for Subject A. The standard deviations are shown in parentheses.	29
Table 5. The thresholds and masking-level differences (MLD) obtained from six trials for each of the 13 signal durations in 68-dB SPL broadband noise for Subject B. The standard deviations are shown in parentheses.	29
Table 6. Estimates of the critical bandwidth (in Hz) for S_0N_0 , $S_{\pi}N_0$, and S_0N_{π} for Subject A and Subject B.	40

INTRODUCTION

The effect of signal duration on the masking-level difference, especially for durations less than 20 ms, has received little experimental attention. This project was designed to investigate the masking-level difference as a function of signal duration. Thresholds for 2- to 100-ms signals were obtained for S_0N_0 , $S_\pi N_0$, and S_0N_π , with emphasis on durations less than 20 ms, and from these data, the $S_\pi N_0$ and S_0N_π masking-level differences were computed. This area of study involves three general areas of auditory research: temporal integration, critical bands, and the masking-level difference. Prior to the literature review on these three topics, a terminology section is included to define the terms and concepts to be discussed.

TERMINOLOGY

Temporal integration refers to the growth of sensation as the duration of the signal is increased to about 200 ms. Both the threshold of audibility and perception of loudness reflect the temporal integration property of the auditory system. The threshold for a signal decreases as duration increases, and a signal is judged to be louder as duration increases.

Perfect power summation (integration) refers to the linear relationship between threshold and duration in which the change in threshold is proportional to the change in duration, i.e., a tenfold decrease in duration results in a 10 dB increase in threshold. Perfect power summation, C , is represented by the formula $I \times t^a = C$, in which I is the threshold intensity level and t is the signal duration. The more general relation between threshold and duration is: $I \times t^a = C$, in which the exponent "a" indicates the rate of temporal integration. In

the instance of perfect power summation, "a" is equal to 1. When the change in threshold intensity level is less than the change in duration, the exponent "a" is less than 1; when the threshold intensity level changes faster than the duration, the exponent "a" is greater than 1. The exponent "a" can vary across the temporal integration function according to the rate of energy integration at different signal durations.

Critical Band refers to the internal bandpass filter that psychoacousticians have proposed to explain various subjective perceptions of auditory phenomena. According to the concept of the critical band, the subjective perception of stimuli with spectra within the frequency region effectively passed by the internal filter is different than the subjective perception of stimuli with spectra outside the frequency region of the bandpass filter.

Masking-Level Difference (MLD) refers to the threshold difference between homophasic (S_0N_0 and $S_\pi N_\pi$) and antiphasic ($S_\pi N_0$ or $S_0 N_\pi$) interaural conditions. For the S_0N_0 condition, both the noise and signal are presented in phase to the ears. For $S_\pi N_0$, the noise is in phase between ears and the signal is 180 degrees (π radians) out of phase between ears. For $S_0 N_\pi$, the signal is in phase between ears and the noise is 180 degrees out of phase between ears. S_0N_0 and $S_\pi N_\pi$ (homophasic) conditions yield higher thresholds than do $S_0 N_\pi$ and $S_\pi N_0$ (antiphasic) conditions. Next are the $S_0 N_\pi$ thresholds, with the $S_\pi N_0$ thresholds yielding the lowest thresholds of the four interaural conditions.

Temporal Integration

In general, as the duration of a pure-tone signal increases, the threshold for that tone decreases. Garner and Miller (1947) investigated the temporal integration of four pure tones (400, 670, 1000, and 1900 Hz) at eight durations (12.5, 25, 50, 100, 200, 500, 1000, and 2000 ms) in broadband noise. Figure 1 illustrates the relationship observed by Garner and Miller between signal duration in milliseconds and masked thresholds in decibels sound pressure level (re: 20 μ P). Over the range of approximately 12.5 to 200 ms, for each tenfold increase in duration of the four pure tones, a 10 dB decrease in threshold occurred. As shown by the function in Figure 1, threshold continues to decrease slightly for durations longer than 200 ms, but the slope, i.e., the change in threshold/the change in signal duration, becomes asymptotic. Temporal integration is essentially complete by 1 s, at which time no further decrease in threshold results from continued increases in duration. Garner and Miller postulated that there is a certain minimal signal duration that is not an effective stimulus for the ear, but that above this minimal duration, temporal integration is linear with log time. According to their findings, this minimal duration or time constant is about 200 ms.

Temporal integration varies according to the spectrum of the signal to be integrated. Garner (1947) reported that the threshold for broadband noise decreases 8 dB for each tenfold increase in duration from 1 to 100 ms, which is in contrast to the perfect power summation that occurs from 12.5 to 200 ms for a 1000-Hz pure tone. The differences among temporal integration functions of various signals are illustrated in Figure 2. Of particular interest are the changes in the

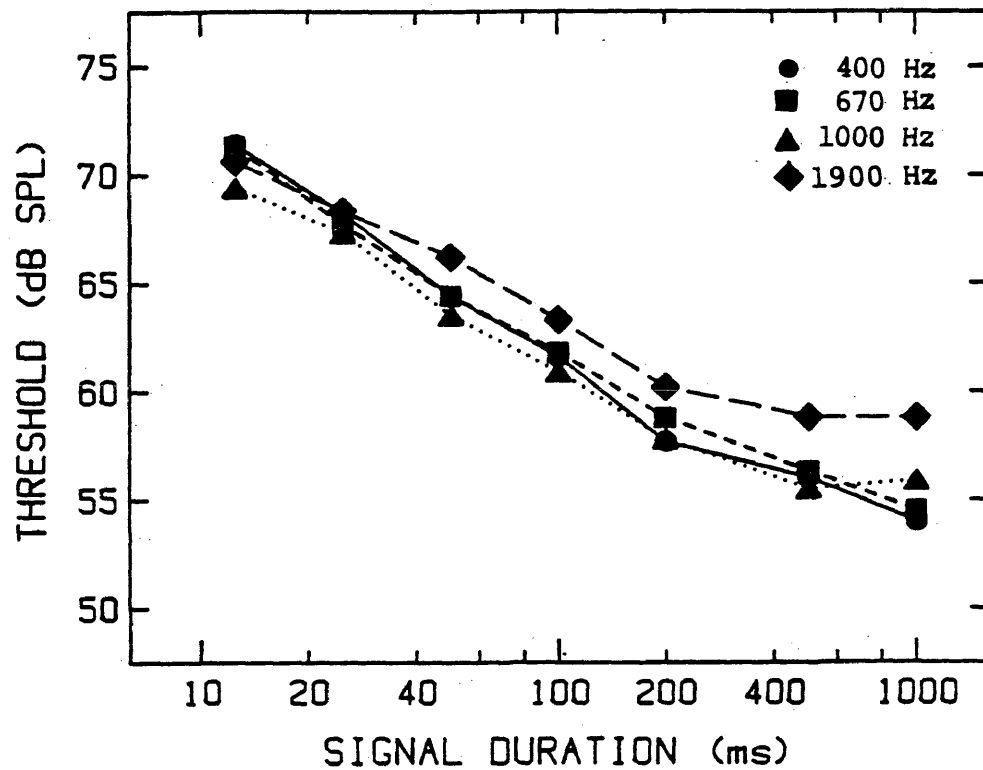


Figure 1. The relation between the masked thresholds (in dB SPL) and signal duration (in ms) for 400-Hz (circles), 670-Hz (squares), 1000-Hz (triangles), and 1900-Hz pure tones (diamonds). (From Garner & Miller, 1947.)

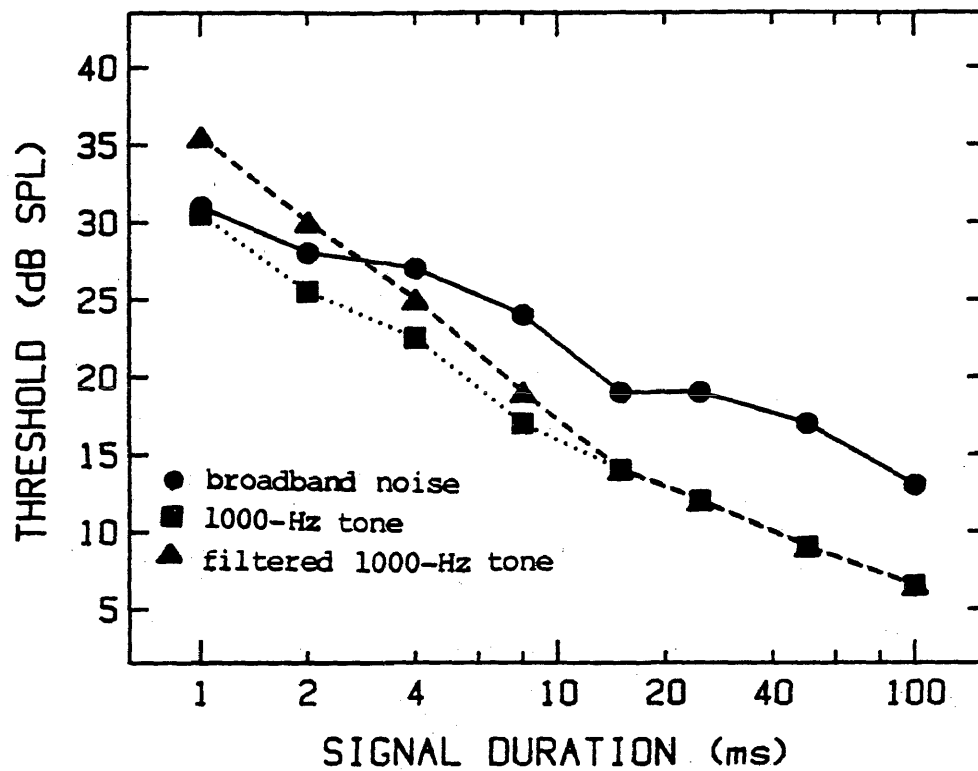


Figure 2. The relation between absolute threshold (in dB SPL) and signal duration (in ms) for broadband noise (circles), a 1000-Hz pure tone (squares), and a filtered 1000-Hz pure tone with a 100-Hz bandwidth (triangles). (From Garner, 1947.)

slopes of the temporal integration functions for different signals at short durations. The slope for a broadband noise function remains a constant 8 dB between 100 and 1 ms. The slope of the 1000-Hz function, however, deviates from linearity at durations shorter than 8 ms, indicating that more energy is required to achieve threshold at short durations than is predicted from perfect power summation. By 1 ms, the 1000-Hz threshold, which is still increasing with decreasing duration, nearly mirrors the broadband noise threshold. Garner used a 1000-Hz filtered tone with a bandwidth of 100 Hz for comparison purposes. The slope of the function for the filtered tone coincides with the slope for the 1000-Hz pure tone over the 15-100 ms interval. The threshold of the filtered tone increases by 17 dB per tenfold decrease in duration below 15 ms.

In addition to investigating temporal integration for signals of different bandwidths, Garner (1947) studied the temporal integration functions for pure tones of different frequencies. Figure 3 illustrates the relationship between absolute threshold and duration for 250- and 4000-Hz signals. The function for 250 Hz reveals thresholds that are much higher than thresholds for both 4000-Hz and for the 1000-Hz signal (as shown in Figure 2). The 250-Hz threshold increases as duration is decreased, but with a more gradual slope compared to the slopes for the 1000 and 4000 Hz functions. At 4 ms, the slope reaches its asymptote, and appears as if it might "fold over" at shorter durations. The thresholds for 4000 Hz are lower than the thresholds for 250 Hz. The thresholds for 4000 Hz are higher than the 1000-Hz thresholds, except at durations less than 2 ms, at which the 4000-Hz thresholds are lower. The temporal integration function for 4000 Hz is different from the

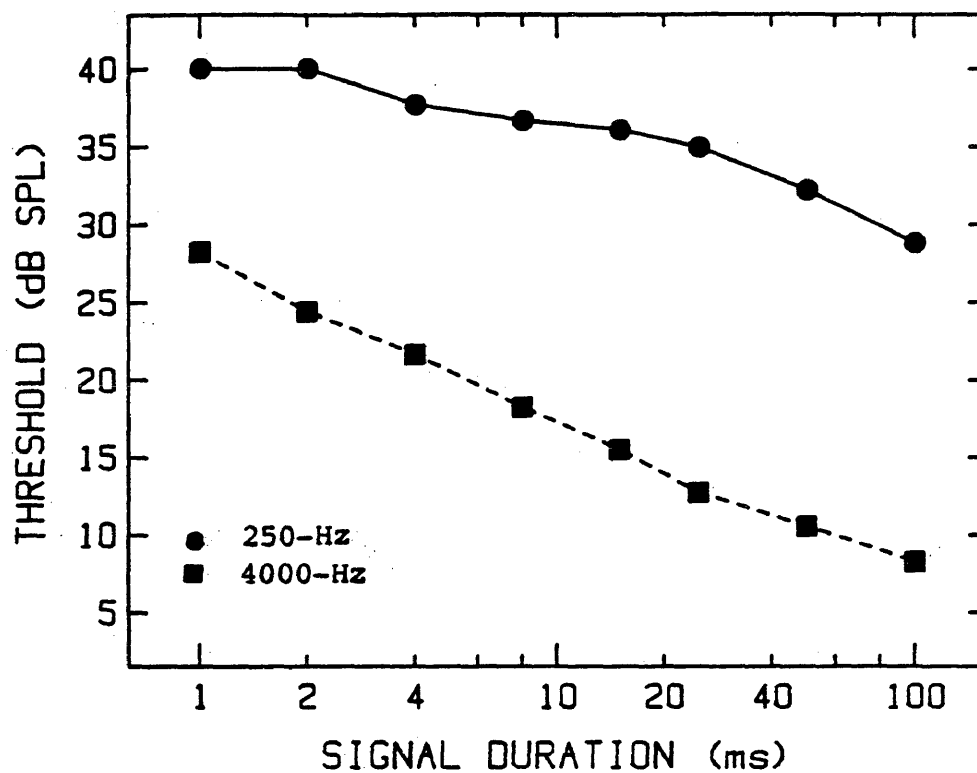


Figure 3. The relation between absolute threshold (in dB SPL) and signal duration (in ms) for 250-Hz (circles) and 4000-Hz pure tones (squares). (From Garner, 1947.)

functions for 250 and 1000 Hz. Instead of being nonlinear at short durations, the slope for 4000 Hz is linear from 1 to 100 ms. Garner attributed the differences in temporal integration of signals of different bandwidths to changes in spectral characteristics that result from decreases in duration. As the duration of a pure tone decreases less than 10 ms, the resulting spectrum has energy spread over a wider range of frequencies than it had at longer durations, until at very short durations (e.g., 1 ms), the "pure tone" is essentially a burst of noise. This effect is demonstrated in Table 1 in which the bandwidth of the signal has been calculated from the signal duration using: $[1000 \text{ (ms)}/\text{signal duration (ms)}]$. Because the energy in the short-duration pure tone is spread over a wide range of frequencies outside the critical band, more energy is required for the signal to be detected. This is because energy outside the critical band does not contribute to threshold (Fletcher, 1940). The slope of the temporal integration function for pure-tone signals, therefore, increases. In contrast, because the bandwidth for broadband noise does not change appreciably as duration decreases, the slope of the temporal integration function for noise remains constant even at very short durations. The effect of frequency spectrum on temporal integration is not fully understood. Although Zwislocki (1961) does not directly refute the Garner (1947) theory, he does suggest that the slope of the temporal integration function at short duration can be explained in other ways, e.g., by neural adaptation (i.e. the decrement in the frequency of neural discharges that takes place during prolonged stimulation). Blodgett, Jeffress, and Taylor (1958), Gassler (1953), Green (1966), and Plomp and Bouman (1959), in contrast, report findings

Table 1. The relations between signal duration, bandwidth and perfect power summation.

Signal Duration (ms)	Bandwidth (Hz)	Computed Perfect Power Summation (dB)
100 (ref)	10.0	0.0
90	11.1	0.5
80	12.5	1.0
70	14.3	1.5
60	16.7	2.2
50	20.0	3.0
45	22.2	3.5
40	25.0	4.0
35	28.6	4.6
30	33.5	5.2
25	40.0	6.0
20	50.0	7.0
15	66.7	8.2
10	100.0	10.0
8	125.0	11.0
6	166.7	12.2
4	250.0	14.0
2	500.0	17.0

that support the Garner theory that integration occurs only within a certain frequency band.

Garner (1947) speculated that differences in thresholds and slopes of the temporal integration functions for 250, 1000, and 4000 Hz are explainable by the natural differential sensitivity of the ear, as illustrated in Figure 4. Because the ear is naturally less sensitive at 250 Hz, more energy is required for threshold than is required for 1000 and 4000-Hz thresholds. The natural filtering of the ear also affects temporal integration at 250 Hz. Based on his data, Garner hypothesized that the critical bandwidth increases at short durations, an hypothesis that is not universally accepted. Assuming the validity of this hypothesis, the resulting spread of energy may stimulate the more sensitive high-frequency regions adjacent to the 250-Hz region. This additional stimulation at short durations for 250 Hz could explain the decrease in slope of the temporal integration function in Figure 3, suggesting that thresholds may actually decrease at even shorter durations.

In summary, the results reported in the early studies of Garner (1947) and Garner and Miller (1947) have been largely supported by more recent investigations (Blodgett et al., 1958; Green, 1966; Plomp & Bouman, 1959). Experimental results suggest that linear integration occurs from about 12.5 to 200 ms. At durations longer than 200 ms, the temporal integration function reaches its asymptote, whereas at durations shorter than about 12.5 ms, the slope of the temporal integration function increases more than is predicted by the various theories of temporal integration. Theories explaining the increase in slope of the function at short durations have not been proven

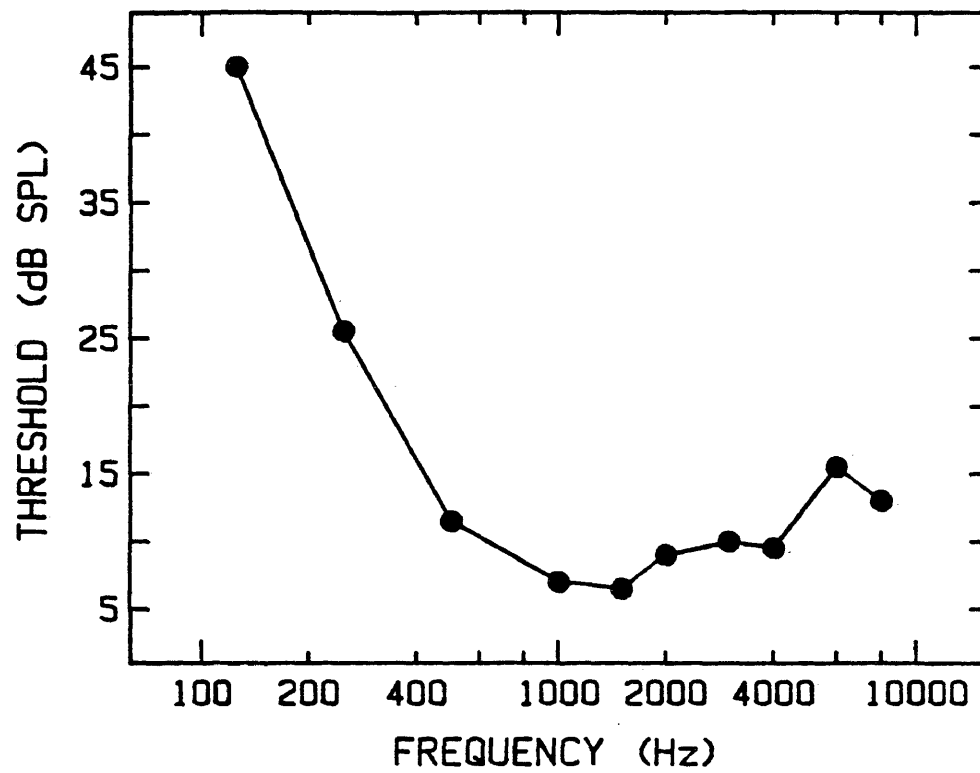


Figure 4. The average minimum audible sound-pressure level curve for a TDH-39 earphone. (From American National Standards Institute, 1969.)

conclusively, but the majority of the research suggests that changes in frequency spectrum probably account for the phenomenon. Furthermore, there is some evidence indicating that the critical bandwidth may be affected by changes in duration (Garner, 1947; Green, 1960; Hamilton, 1957; Plomp & Bouman, 1959).

Critical Bands

The critical band has been proposed to explain various subjective perceptions of auditory phenomena. Swets, Green, and Tanner (1962, cited by Scharf, 1970) suggested that the critical band represents an internal bandpass filter. Because of the internal filtering that occurs in the auditory system, the subjective perception of stimuli with spectra within the frequency region effectively passed by the internal filter is different than the subjective perception of stimuli with spectra outside of the frequency region of the bandpass. Physiologically, the critical band mechanism is thought to exist peripherally, probably in the cochlea (von Békésy, 1960, van den Brink, 1964; Zwislocki, 1965; as cited by Scharf, 1970). According to Scharf, the role of central or cognitive factors on the internal filtering mechanism is unclear. The critical band may be one part of a multi-stage filtering process in the auditory system, or it may account for the entire perceptual process.

Empirically, the critical band refers to that bandwidth at which subjective responses abruptly change. For example, narrow-band masking experiments demonstrate that as the noise bandwidth is increased up to the critical band, a pure tone becomes more difficult to detect, but that increases in the noise bandwidth beyond the critical band do not affect the detectability of the tone. The critical band is a directly

measured value. The critical ratio, an indirectly-derived value, is used to describe the signal-to-noise ratio for a pure tone just masked by a broadband noise (Scharf, 1970). Estimates of the critical band are up to 2.5 times larger than estimates of the critical ratio. Results from several experiments suggest that the critical ratio is a relatively unstable measure, thereby making reliable and valid estimates of the critical band somewhat difficult. In spite of the variability, the critical ratio is used to compare critical bands as a function of frequency.

Critical bands have been studied utilizing the following types of experiments: loudness summation, narrow-band masking, two-tone masking, threshold, phase sensitivity, and harmonic discrimination. The findings of all these experiments suggest, within limits, that the width of a critical band is dependent upon the center frequency and is independent of sound-pressure level. The data in Table 2 illustrate the relationship between critical bandwidth and center frequency.

Temporal Integration and Critical Bands

Few studies have dealt primarily with describing the effect that changes in signal duration have on critical bands. Several theories concerning the relationship between temporal integration and critical bands have been developed from inferences based on threshold integration functions reported in the literature. Scharf (1970) has provided a synopsis of the various theories regarding the duration-critical band relationship, based on the findings of a number of investigations. Scharf separates these studies into the following four groups.

Table 2. The relationship between critical bandwidth and center frequency. (From Scharf, 1970.)

Center Frequency (Hz)	Critical Bandwidth (Hz)
150	100
250	100
350	100
450	100
570	120
700	140
840	150
1000	160
1170	190
1370	210
1600	240
1850	280
2150	320
2500	380
2900	450
3400	550
4000	700
4800	900
5800	1100
7000	1300
8500	1800

1. One group of studies that manipulated the duration of narrow and broadband maskers supports the position that as the stimulus duration decreases, the critical bandwidth increases (Elliott, 1965; Feldtkeller & Oettinger, 1956; Garner, 1947; Green, 1960; Hamilton, 1957; Miller, 1948; Miskolczy-Fodor, 1959; Scholl, 1962b; Zwicker & Wright, 1963, as cited by Scharf, 1970). Scholl found that the critical band for a 2000-Hz pure tone increased from almost 300 Hz, its steady state value at 300 ms, to 750 Hz at 3 ms. The characteristic increase in the slope of the temporal integration function at short durations suggests that although the critical band may become wider at short durations, the change in critical bandwidth is not equivalent to the increase in the bandwidth of the signal.
2. Another possible explanation of the relationship between critical bands and duration is that at short durations, the critical band ceases to exist. In a study by Scholl (1962a, cited by Scharf, 1970), the duration and bandwidth of the signal was varied. The results of this experiment indicated that the critical band widens with decreasing duration until 3 ms, at which the critical band disappears.
3. A third possible relationship is that the critical band is narrower at short durations. In a study by Plomp and Bouman (1959), thresholds began to increase more than predicted by perfect power summation at relatively long durations (e.g. 10 to 50 ms). Because the energy of a signal of 10 to 50 ms is within the normal critical bandwidth, Scharf interpreted the

Plomp and Bouman results to indicate that critical bands become narrower at short durations.

4. A fourth hypothesis, discussed by Scharf, (1970), involves the possibility that the detection of very short signals with broadband spectra may involve multiple static critical bands, as opposed to dynamic critical bands. As the spectral energy of short duration tones spreads over a wide range of frequencies outside the static critical band for the tone, the adjacent critical bands may become involved.

Studies utilizing the masking-level difference paradigm have proposed some interesting possibilities concerning temporal integration and critical bands. In general, the masking-level difference is about 2 to 4 dB larger at 10 ms than it is at 100 ms (Blodgett et al., 1958; Green, 1966; Wilson & Fowler, 1985). This effect is demonstrated in Figure 5, in which masked thresholds are shown as a function of the 500-Hz signal duration for different interaural conditions. The slopes of the functions for SS_0N_0 and $S_{\pi}N_0$ conditions are roughly parallel to each other from 500 to 50 ms, at which a sharp increase in slope occurs. Another increase in slope occurs at 15 ms, at which the slope increases more for S_0N_0 conditions (-9 dB) than for $S_{\pi}N_0$ conditions (-7 dB). Wilson and Fowler investigated the effect of duration on the 500-Hz masking-level difference for durations from 2 to 128 ms. Figure 6 illustrates the relationship between threshold and duration for S_0N_0 and $S_{\pi}N_0$ conditions for the interval from 2 to 100 ms. From 10 to 100 ms, nearly perfect power summation occurred for the $S_{\pi}N_0$ condition, e.g., 10 dB more energy was required to maintain threshold at 10 ms than was needed at 100 ms. In contrast, the slope for the S_0N_0

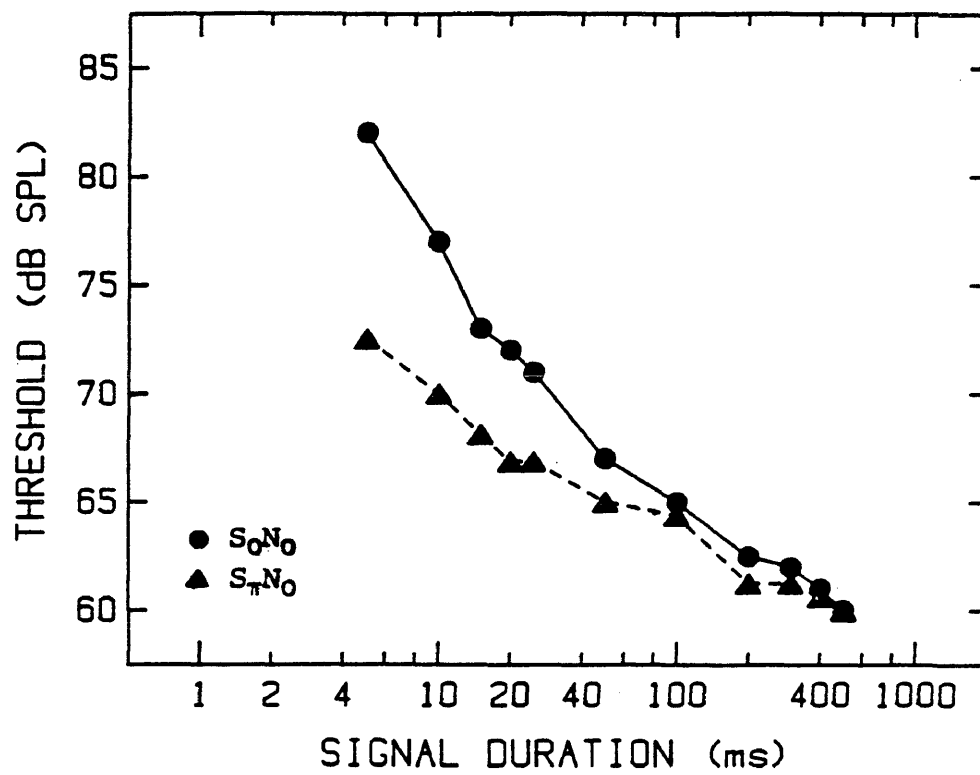


Figure 5. The relation between masked thresholds (in dB SPL) and the 500-Hz signal duration (in ms) for SoNo (circles) and SpNo (triangles). (From Blodgett, Jeffress & Taylor, 1958.)

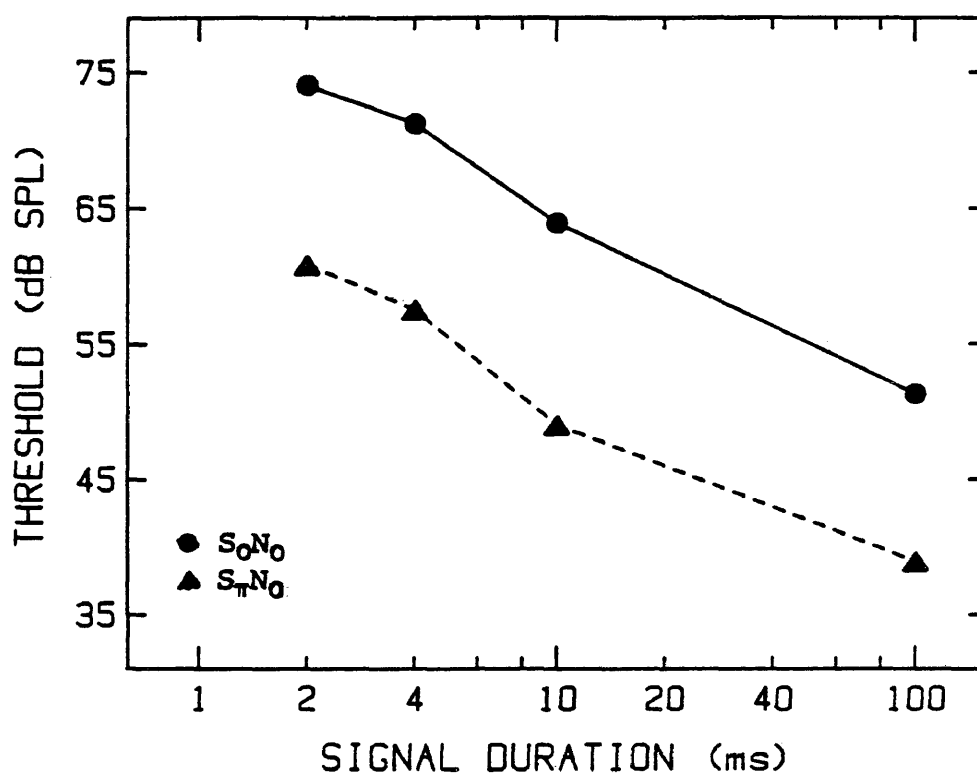


Figure 6. The relation between masked thresholds (in dB SPL) and the 500-Hz signal duration (in ms) for S_{oN_0} (circles) and $S_{\pi N_0}$ (triangles). (From Wilson & Fowler, 1985.)

condition was steeper, indicating that more energy (+12 dB) was required to maintain threshold for S_0N_0 than was required for $S_{\pi}N_0$. As a result of these temporal integration differences, the masking-level difference increased by 2.3 dB as duration decreased from 100 to 10 ms. From 10 to 2 ms, however, the slope for S_0N_0 was more gradual than the slope for $S_{\pi}N_0$. The resulting masking-level difference decreased by 1.7 dB as duration decreased from 10 to 2 ms. Figure 7 gives the mean masking-level differences obtained for the following four signal durations: 2, 4, 10, and 100 ms.

The reason for the differences in slopes of the temporal integration functions between S_0N_0 and $S_{\pi}N_0$ conditions is not known. Several possible explanations have been discussed in the literature. Wilson and Fowler (1985) discussed the possibility that "the auditory system may require a minimal sampling interval over which to extract and interpret most efficiently phase information from binaural inputs." Data from 100- μ s low-pass clicks (Yost & Dolan, 1978; Yost & Silva, 1977) revealed a large (11-15 dB) masking-level difference, thereby arguing against this line of reasoning. Another possibility is that the critical bands are differentially dynamic at short durations for S_0N_0 and $S_{\pi}N_0$ conditions. This idea would apply both to theories that suggest the existence of wider than normal critical bands at short durations and to those that suggest the existence of narrower than normal critical bands at short durations. Wilson and Fowler agreed with Scharf (1970) and suggested as other possibilities that (1) the critical band concept may not apply for signals of very short duration, and (2) the detection of very short signals may involve multiple static critical bands, as opposed to dynamic critical bands.

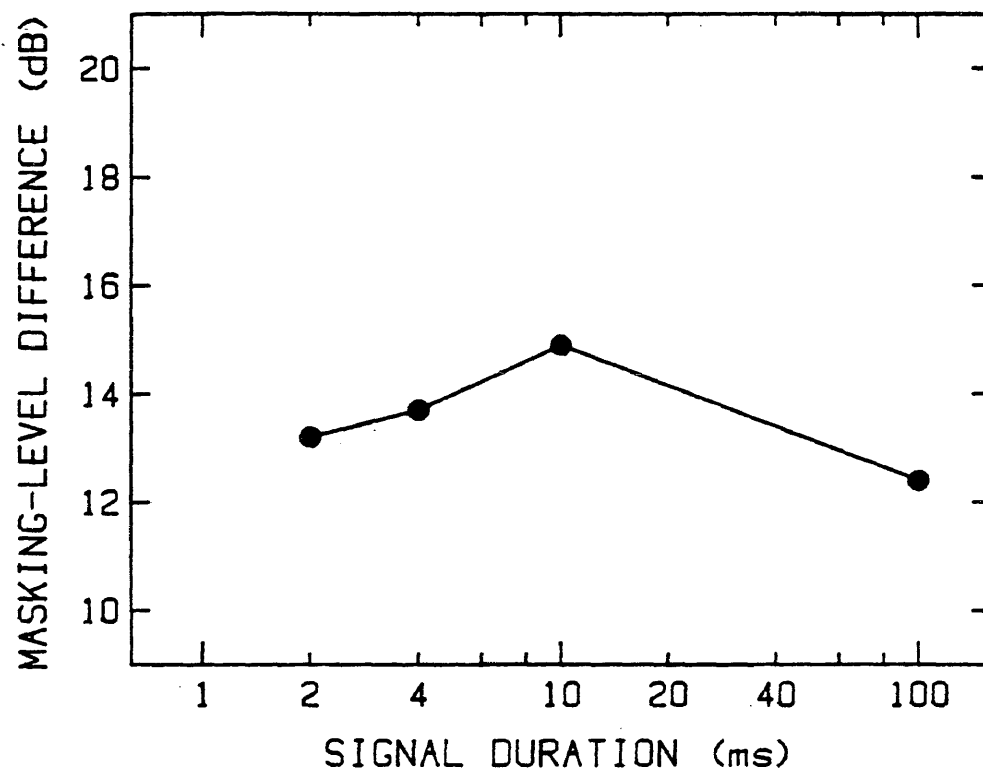


Figure 7. The mean masking-level differences (in dB) obtained for four 500-Hz signal durations (in ms). (From Wilson & Fowler, 1985.)

To summarize, the literature on masking-level differences has shown differential integration of energy for S_0N_0 and $S_{\pi}N_0$ conditions, especially as duration is decreased less than 20 ms. The conclusions of most of the studies suggest that the differences may relate to the underlying relationship between temporal integration and critical bands. This relationship, however, has not been conclusively established, and remains a controversial topic in psychoacoustics. The purpose of the present experiment is to examine more closely temporal integration for S_0N_0 and $S_{\pi}N_0$ conditions, by observing threshold behavior at a greater number of durations than were previously studied. The resulting temporal integration functions, therefore, will provide a more detailed description of threshold behavior for S_0N_0 and $S_{\pi}N_0$ conditions as duration is decreased, particularly below 20 ms. From these data, inferences may be made regarding critical band theory, and insights may be gained into the analysis of temporal information by the auditory system. In this experiment, the masked thresholds for S_0N_0 , $S_{\pi}N_0$, and S_0N_{π} for 13 signal durations from 2 to 100 ms were obtained.

METHODS

Subjects

Two female subjects participated. Both subjects had normal hearing (less than 25 dB HL, ANSI, 1969) at 500 Hz. Subject A (age 25:10 years) had normal hearing from 250 to 8000 Hz, and Subject B (age 24:10 years) had mild sensory hearing loss from 2000 through 8000 Hz (25- to 40-dB HL air and bone conduction pure-tone thresholds). All testing was conducted in a sound booth (IAC, Model 1203A).

Instrumentation

The 500-Hz signal was synthesized and switched digitally (DEC, Model 11/23) to begin at a positive zero crossing. The signal was put out by a 12-bit digital-to-analog converter (20,000 Hz), and passed through both a smoothing filter with a 60-dB/octave rejection rate (Reticon, Model 5609) and a programmable attenuator (Grason-Stadler, Model 1292). A microcomputer (Hewlett-Packard, Model 85) controlled the programmable attenuator and the 11/23 computer that generated the signals. Additionally, the microcomputer recorded and stored the responses of the subjects. An audiometer (Grason-Stadler, Model 10) generated the broadband noise (presented continuously at 68-dB SPL), mixed and phase aligned the signal and noise for the S_0N_0 , $S_\pi N_0$, and S_0N_π conditions, and fed the stimuli to TDH-50P earphones encased in MX-41/AR cushions. The earphones were matched for frequency response and phase characteristics. Throughout the experiment, the level of the 500-Hz signal was monitored constantly on an oscilloscope (Tektronix, Type 5113) and the level of the noise was monitored on a VU meter.

Thirteen signal durations were studied (2, 4, 6, 8, 10, 15, 20, 25, 30, 40, 60, 80, and 100 ms). The 11/23 computer shaped the signal onset and offset with a cosine squared routine that produced a trapezoidal signal envelope with 1-ms rise-fall times. Thus, the 2-ms signal had a 1-ms rise-fall time with no plateau. A storage oscilloscope (Tektronix, Type 5113) was utilized to measure the peak-to-peak voltages of the 13 signals. The voltages were identical for the 4- through 100-ms signals. Because of the signal envelope, the peak-to-peak voltage of the 2-ms signal was 6 dB lower than the peak-

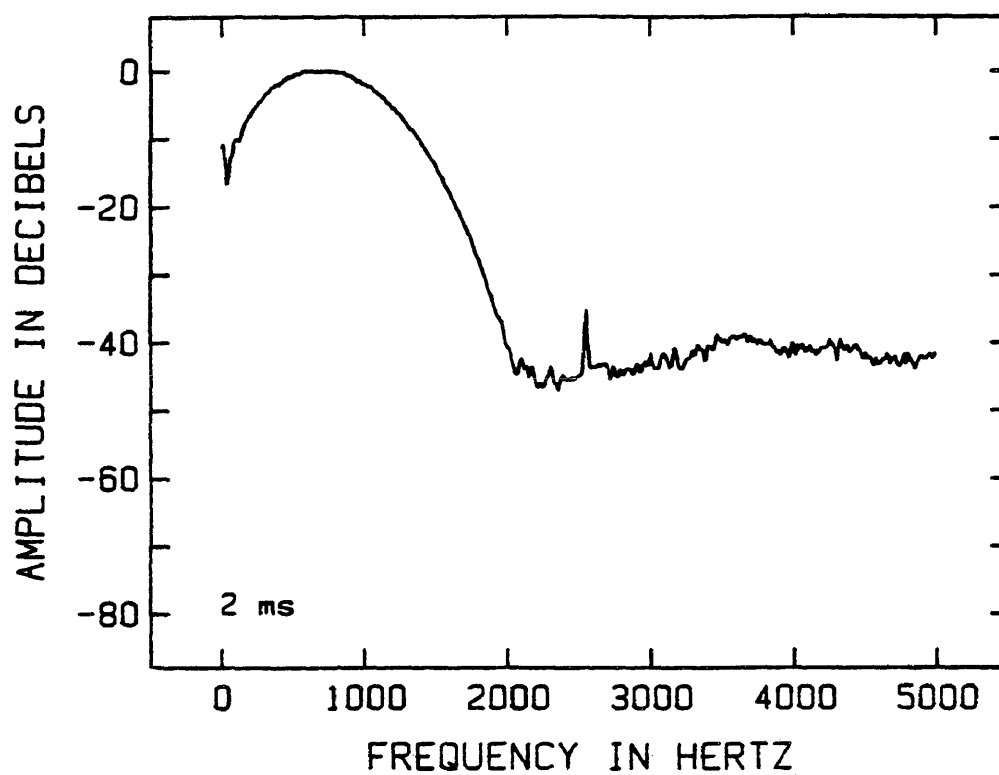


Figure 8a. The acoustic power spectrum of the 2 ms, 500-Hz signal determined from 32 samples of the signal on a NBS-9A coupler and a spectrum analyzer (Bruel & Kjaer, Type 2033).

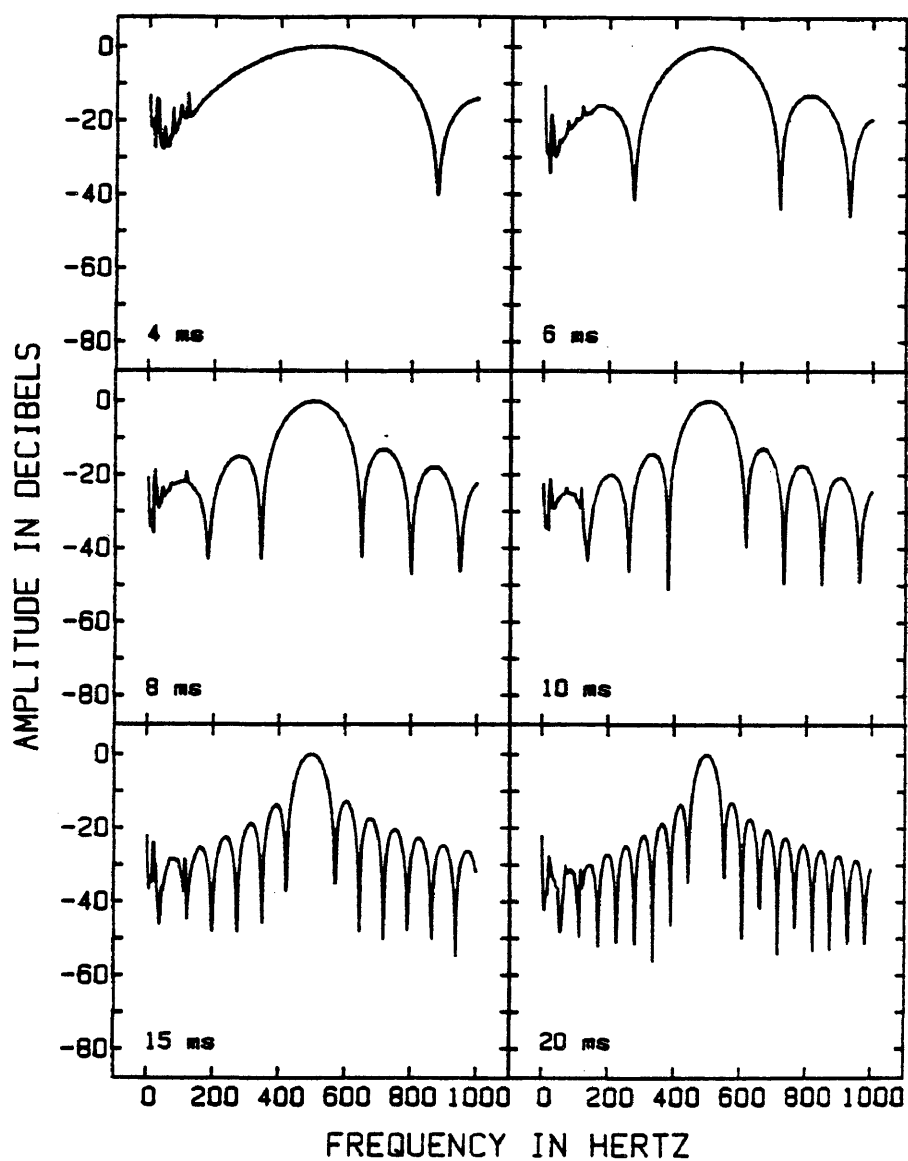


Figure 8b. The acoustic power spectra of the 4- through 20-ms, 500-Hz signals determined from 32 samples of each signal on a NBS-9A coupler and a spectrum analyzer (Bruel & Kjaer, Type 2033).

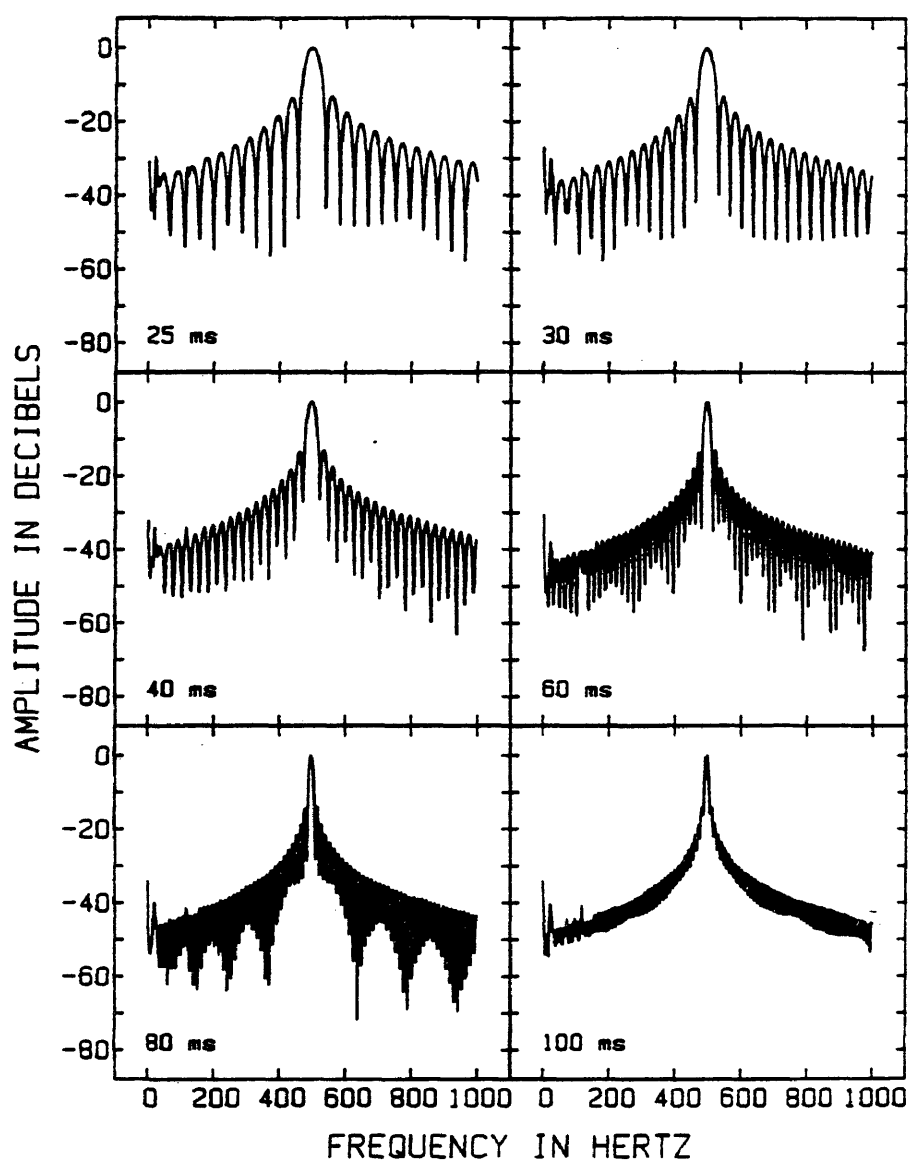


Figure 9. The acoustic power spectra of the 25- through 100-ms, 500-Hz signals determined from 32 samples of each signal on a NBS-9A coupler and a spectrum analyzer (Bruel & Kjaer, Type 2033).

Table 3. The half-power points or the 3-dB down points of the respective spectrum of the 13 signal durations. The 3-dB bandwidth also is listed.

Signal Duration (ms)	Low-frequency Cutoff (Hz)	High-frequency Cutoff (Hz)	3-dB Bandwidth (Hz)
2	175	825	650
4	355	680	325
6	410	600	190
8	435	570	135
10	450	555	105
15	467	532	65
20	475	525	50
25	480	520	40
30	485	515	30
40	485	512	25
60	492	508	16
80	495	505	10
100	595	505	10

correct, then the next signal was presented at a lower level. In contrast, if the response to the second signal were incorrect, then the next signal was presented at a higher level. Changes in the sign of the response tracking constituted a reversal that defined one extreme of an excursion. Threshold (70.7%) was defined as the mean of the excursion midpoints following the first two reversals with the 2-dB steps. Usually 24-30 reversals were completed during a run. Six trials were conducted, with each trial consisting of 13 randomized runs corresponding to the 13 durations used in the experiment. Each run consisted of the S_0N_0 , $S_\pi N_0$, and S_0N_π conditions, and lasted approximately 21 minutes (about 7 minutes per condition). The order of the three conditions in each run were randomized. Each subject listened for a total of about 46 hours, including practice, during the experiment, over a 6- to 7-week interval.

RESULTS

The individual data for Subjects A and B are presented in Tables 4 and 5, respectively, and in Figure 10 (thresholds) and Figure 11 (masking-level differences). Figure 10 illustrates the temporal integration functions for S_0N_0 , $S_\pi N_0$, and S_0N_π conditions. The circles represent S_0N_0 thresholds, whereas the triangles and rectangles represent $S_\pi N_0$ and S_0N_π thresholds, respectively. The dotted lines represent the thresholds predicted by perfect power summation, using the respective 100 ms thresholds as the reference. The data for Subject A are displayed in the top panel, the data for Subject B are displayed in the middle panel, and the mean data are displayed in the bottom panel. Consider first the S_0N_0 thresholds for the two subjects. The temporal integration function for Subject A (top panel) reveals

Table 4. The thresholds and masking-level differences (MLD) for Subject A obtained from six trials for each of the 13 signal durations in 68-dB SPL broadband noise. The standard deviations are shown in parentheses.

Signal Duration (ms)	Threshold (dB SPL)			MLD (dB)	
	S_0N_0	$S_{\pi}N_0$	S_0N_{π}	$S_{\pi}N_0$	S_0N_{π}
2	78.8 (0.7)	64.3 (1.0)	67.1 (0.8)	14.5	11.7
4	73.7 (0.7)	59.1 (1.4)	60.1 (1.5)	14.6	13.6
6	71.4 (0.9)	54.2 (1.0)	56.4 (1.0)	17.3	15.0
8	69.7 (1.3)	52.4 (0.8)	54.6 (0.7)	17.4	15.1
10	67.4 (0.9)	49.7 (0.9)	53.8 (0.8)	17.7	13.6
15	63.7 (0.7)	48.5 (2.1)	50.5 (1.0)	15.3	13.2
20	60.8 (0.9)	45.3 (1.8)	47.8 (1.0)	15.5	13.0
25	59.9 (0.2)	45.4 (0.3)	46.9 (1.7)	14.5	13.1
30	58.5 (1.1)	43.4 (1.2)	46.3 (1.6)	15.1	12.2
40	58.4 (1.2)	42.6 (1.0)	45.2 (1.3)	15.8	13.1
60	54.8 (1.1)	41.9 (0.6)	43.2 (1.0)	12.9	11.5
80	53.6 (1.6)	40.3 (0.8)	41.6 (1.1)	13.3	12.0
100	53.7 (1.3)	39.7 (0.9)	41.7 (1.1)	14.0	12.0

Table 5. The thresholds and masking-level differences (MLD) for Subject B obtained from six trials for each of the 13 signal durations in 68-dB SPL broadband noise. The standard deviations are shown in parentheses.

Signal Duration (ms)	Threshold (dB SPL)			MLD (dB)	
	S_0N_0	$S_{\pi}N_0$	S_0N_{π}	$S_{\pi}N_0$	S_0N_{π}
2	78.8 (0.6)	65.4 (0.5)	67.9 (1.1)	13.4	10.8
4	73.4 (1.4)	58.8 (0.9)	62.4 (1.5)	14.6	11.0
6	70.0 (1.0)	56.0 (1.3)	58.3 (1.1)	14.0	11.7
8	68.0 (0.7)	50.6 (3.1)	53.3 (1.9)	17.3	14.7
10	66.4 (0.8)	51.5 (1.1)	54.1 (2.2)	14.9	12.2
15	64.1 (1.5)	49.0 (1.1)	50.5 (1.7)	15.1	13.6
20	61.4 (0.7)	48.2 (0.8)	48.2 (1.0)	13.3	13.2
25	59.6 (1.0)	45.6 (0.8)	47.4 (1.1)	13.9	12.2
30	59.1 (0.4)	44.6 (1.4)	46.7 (0.9)	14.5	12.5
40	57.8 (1.4)	43.8 (0.7)	45.6 (1.5)	14.0	12.2
60	55.8 (2.0)	42.0 (0.4)	44.3 (1.8)	13.8	11.5
80	54.9 (1.4)	41.1 (0.7)	43.4 (0.6)	13.8	11.6
100	54.7 (1.2)	41.1 (0.6)	44.2 (1.3)	13.7	10.5

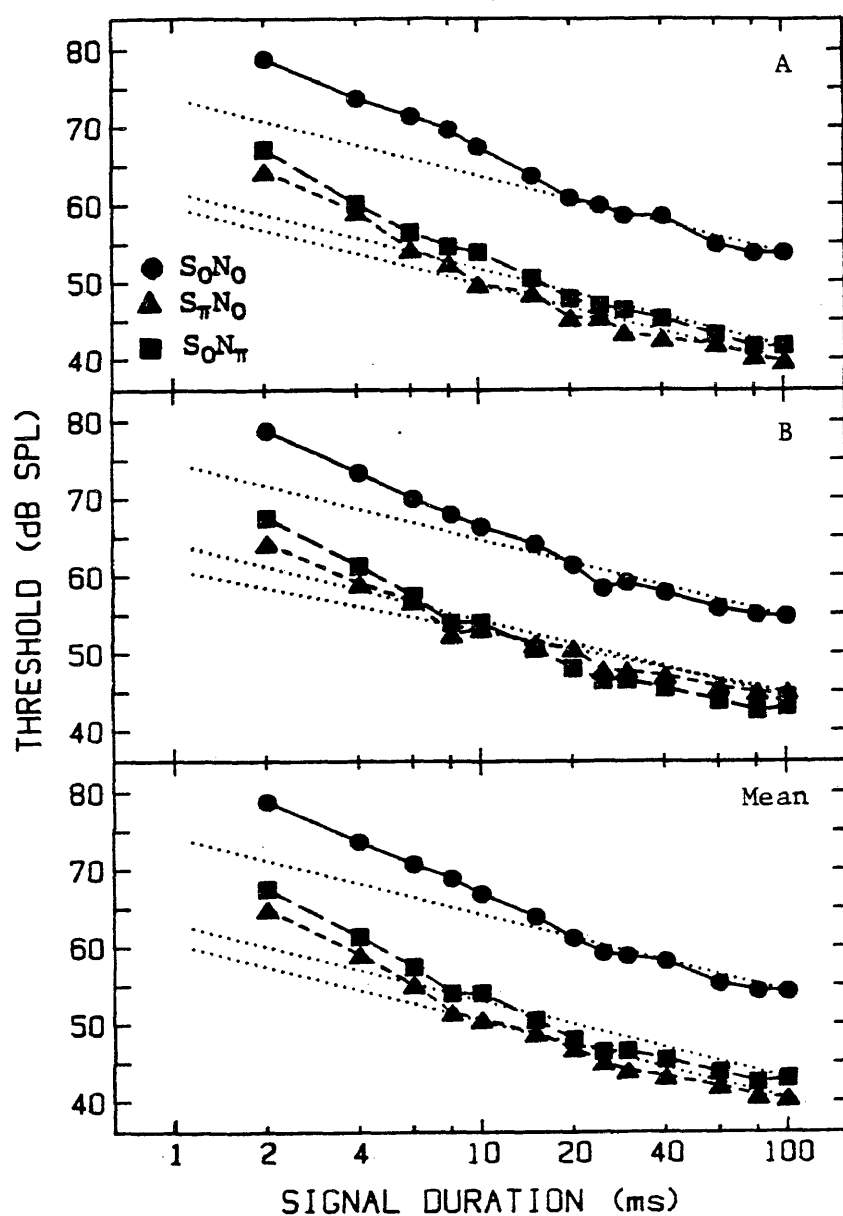


Figure 10. The individual and mean 500-Hz thresholds (in dB SPL) for S_oN_o (circles), $S_{\pi}N_o$ (triangles), and S_oN_{π} (rectangles) obtained for the 13 durations (in ms) in 30.7-dB pressure-spectrum level, broadband noise. The thresholds for Subject A and Subject B are presented in the top and middle panels, respectively. The mean thresholds are presented in the bottom panel.

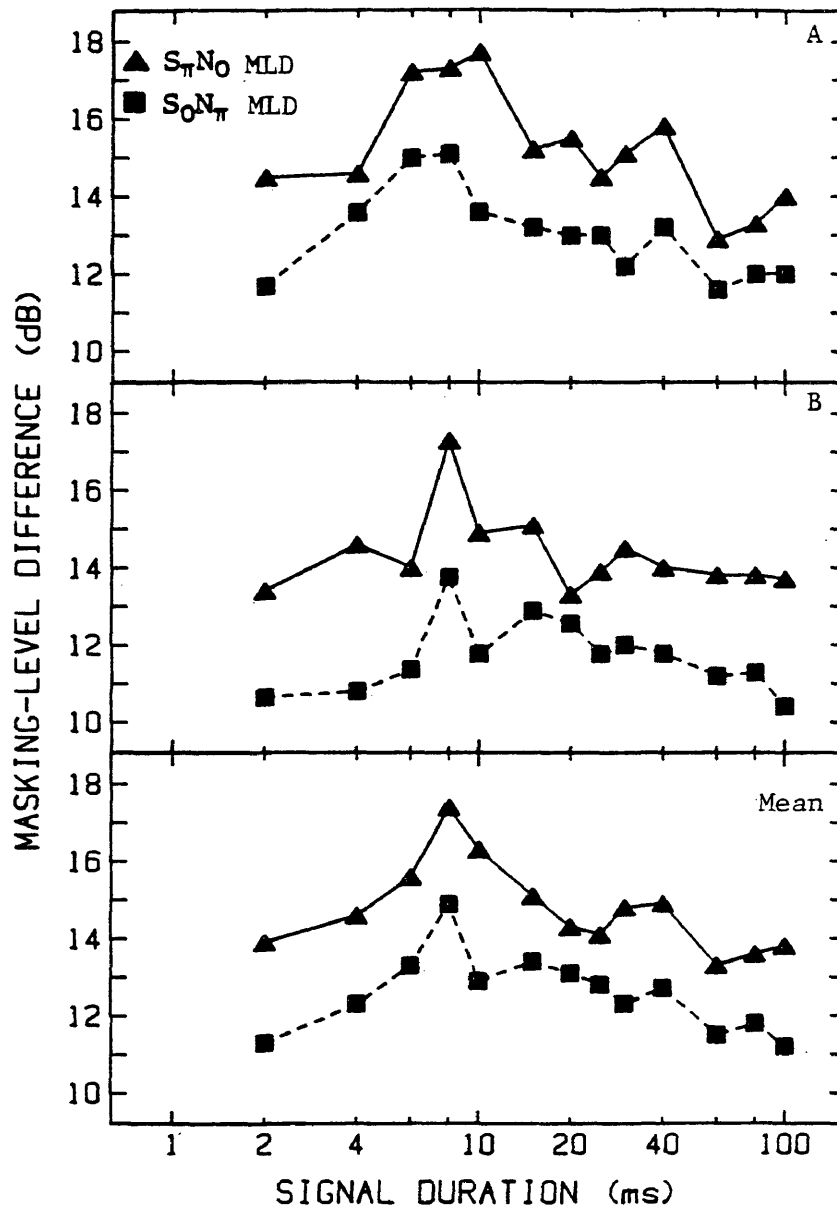


Figure 11. The $S_{\pi}N_0$ (triangles) and S_0N_{π} (rectangles) 500-Hz masking-level differences (in dB) obtained for the thirteen durations (in ms) in 30.7-dB pressure-spectrum level, broadband noise for Subject A (top) and Subject B (middle). The mean masking-level differences are illustrated in the bottom panel.

that as duration decreases from 100 to 20 ms, the thresholds increase as predicted by perfect power summation (represented by the dotted line). For Subject B, S_0N_0 thresholds closely match the predicted thresholds for the 15- to 100-ms interval. At durations shorter than 20 ms for Subject A and 15 ms for Subject B, the threshold increase is greater than that predicted by perfect power summation. The slopes of the measured and predicted functions become increasingly divergent, until at 2 ms, there are differences between the predicted and measured thresholds of 8.1 and 7.1 dB for Subjects A and B, respectively.

Consider next the $S_{\pi}N_0$ thresholds for the two subjects. Perfect power summation occurs from 100 to 10 ms for Subject A, and from 100 to 8 ms for Subject B. As duration is decreased below these breakpoints, i.e., the duration at which the measured threshold function deviates from the predicted threshold function, more energy is required to maintain threshold than is predicted by perfect power summation. The S_0N_{π} temporal integration function for Subject B reveals that perfect power summation occurs from 100 to 15 ms, presenting a breakpoint in the function that is between the breakpoints for S_0N_0 and $S_{\pi}N_0$. In contrast, the function for Subject B reveals that $S_{\pi}N_0$ and S_0N_{π} have the same points of departure from perfect power summation.

Figure 11 presents the $S_{\pi}N_0$ masking-level difference (triangles) and the S_0N_{π} masking-level difference (rectangles) as a function of signal duration for Subject A (top panel) and Subject B (middle panel). The mean $S_{\pi}N_0$ and S_0N_{π} masking-level differences are illustrated in the bottom panel. The masking-level differences at the extremes of the duration continuum for Subject A are nearly identical, (14.5 dB at 2

ms, 14.0 dB at 100 ms) and are relatively small compared to the masking-level differences that occur for the 6- to 10-ms interval (17.2 to 17.7 dB). The masking-level differences for Subject B demonstrate similar increases from 13.4 and 13.7 dB at 2 and 100 ms, to 17.3 dB at 8 ms. The masking-level differences suggest that the maximum divergence of the slopes for S_0N_0 and $S_{\pi}N_0$ (and S_0N_{π}) occurs between 6 and 10 ms for Subject A and at 8 ms for Subject B.

DISCUSSION

For the three binaural listening conditions, both subjects required considerably more energy to maintain threshold at 2 ms than at 100 ms. The data in Tables 4 and 5 revealed that the threshold differences between 2 and 100 ms were 24.6 to 26.0 dB (Subject A) and 23.7 to 24.3 dB (Subject B) for S_0N_0 , $S_{\pi}N_0$, and S_0N_{π} . These threshold differences are similar to the 22 to 22.6 dB differences between 2- and 100-ms signal thresholds for S_0N_0 and $S_{\pi}N_0$ reported by Wilson and Fowler (1985). In every condition, the threshold difference between 2 and 100 ms exceeds the 17 dB difference predicted by perfect power summation (re: the 100-ms threshold).

In the results section, the threshold data were plotted in a traditional format in Figure 10, in which threshold (dB SPL) was shown as a function of signal duration (ms). The same threshold data were transformed by subtracting the thresholds predicted from perfect power summation (using the 100-ms threshold as the reference) from the measured thresholds. The difference thresholds or the constant energy thresholds (dB) are presented in Figure 12 as a function of signal duration for S_0N_0 (top panel), $S_{\pi}N_0$ (middle panel), and S_0N_{π} (bottom panel). The dotted line represents the threshold increase predicted by

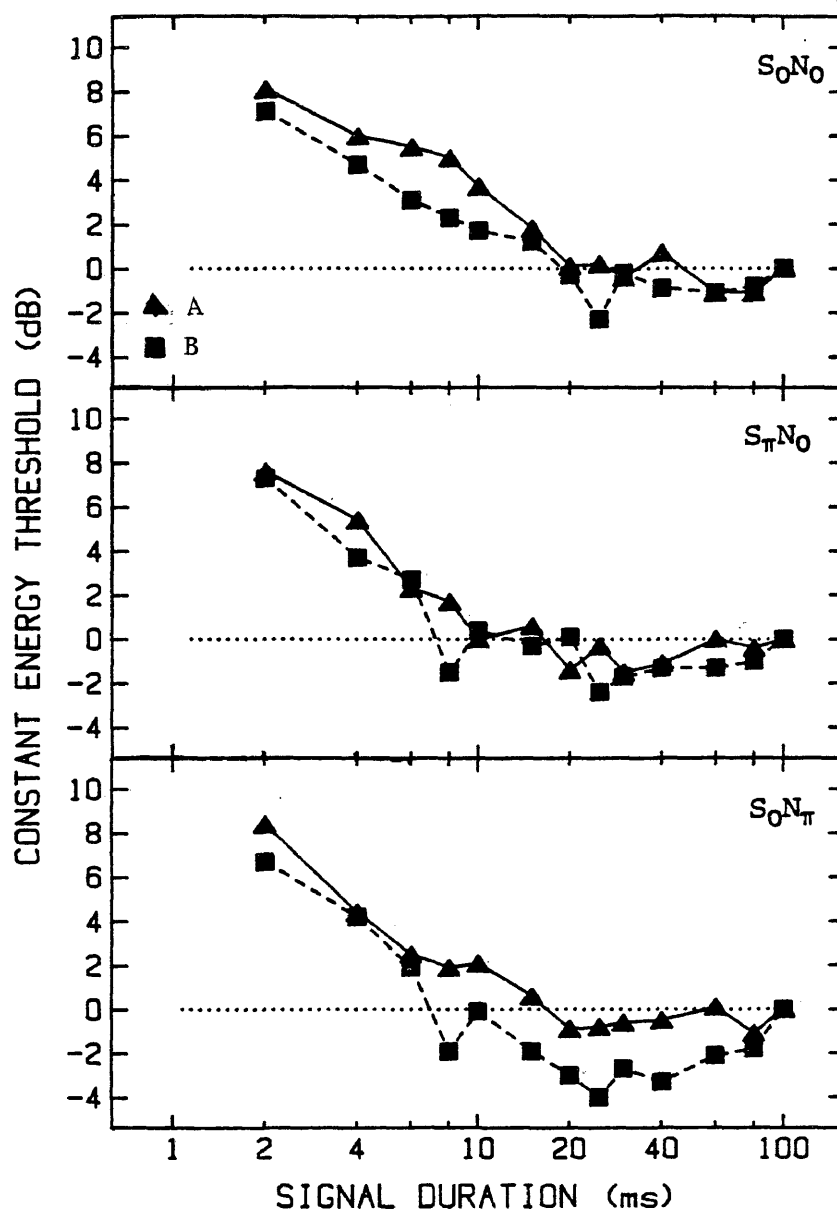


Figure 12. The thresholds (in dB), corrected for perfect power summation (see Table 2), as a function of the 500-Hz signal duration for S_0N_0 (top), $S_\pi N_0$ (middle), and S_0N_π (bottom). The dotted line represents perfect power summation. Thresholds for Subject A and Subject B are represented by triangles and rectangles, respectively.

perfect power summation. The thresholds for Subject A are illustrated by triangles, whereas the thresholds for Subject B are represented by rectangles. For Subject A, the thresholds for S_0N_0 , $S_{\pi}N_0$, and S_0N_{π} are relatively consistent with the predicted thresholds until 20, 10, and 15 ms, respectively. The functions become increasingly divergent from the predicted functions as duration is decreased, until at 2 ms, the thresholds are 7.6 to 8.4 dB higher than the predicted thresholds. The thresholds for Subject B are relatively consistent with the predicted thresholds until 15 ms for S_0N_0 , and until 8 ms for $S_{\pi}N_0$ and S_0N_{π} , at which the threshold increase is greater than predicted. At 2 ms, the thresholds are 6.7 to 7.3 dB higher than the predicted thresholds. The differences between the predicted and measured thresholds at 2 ms for the two subjects are slightly greater than the 5 to 5.6 dB differences for 2-ms S_0N_0 and $S_{\pi}N_0$ signals reported by Wilson and Fowler (1985).

Figure 13 illustrates the relationship between the measured and predicted thresholds in yet another way, by presenting bivariate plots of the measured thresholds (ordinate) and predicted thresholds (abscissa) for Subject A (top panel) and Subject B (bottom panel). The dotted lines represent the thresholds predicted by perfect power summation. The circles represent S_0N_0 thresholds, whereas the triangles and rectangles represent $S_{\pi}N_0$ and S_0N_{π} thresholds, respectively. Deviations above the dotted line indicate that the measured thresholds for the shorter duration signals are higher in sound-pressure level than the predicted thresholds.

The differences in the slopes of the temporal integration functions for S_0N_0 and $S_{\pi}N_0$ are reflected by the changes in masking-

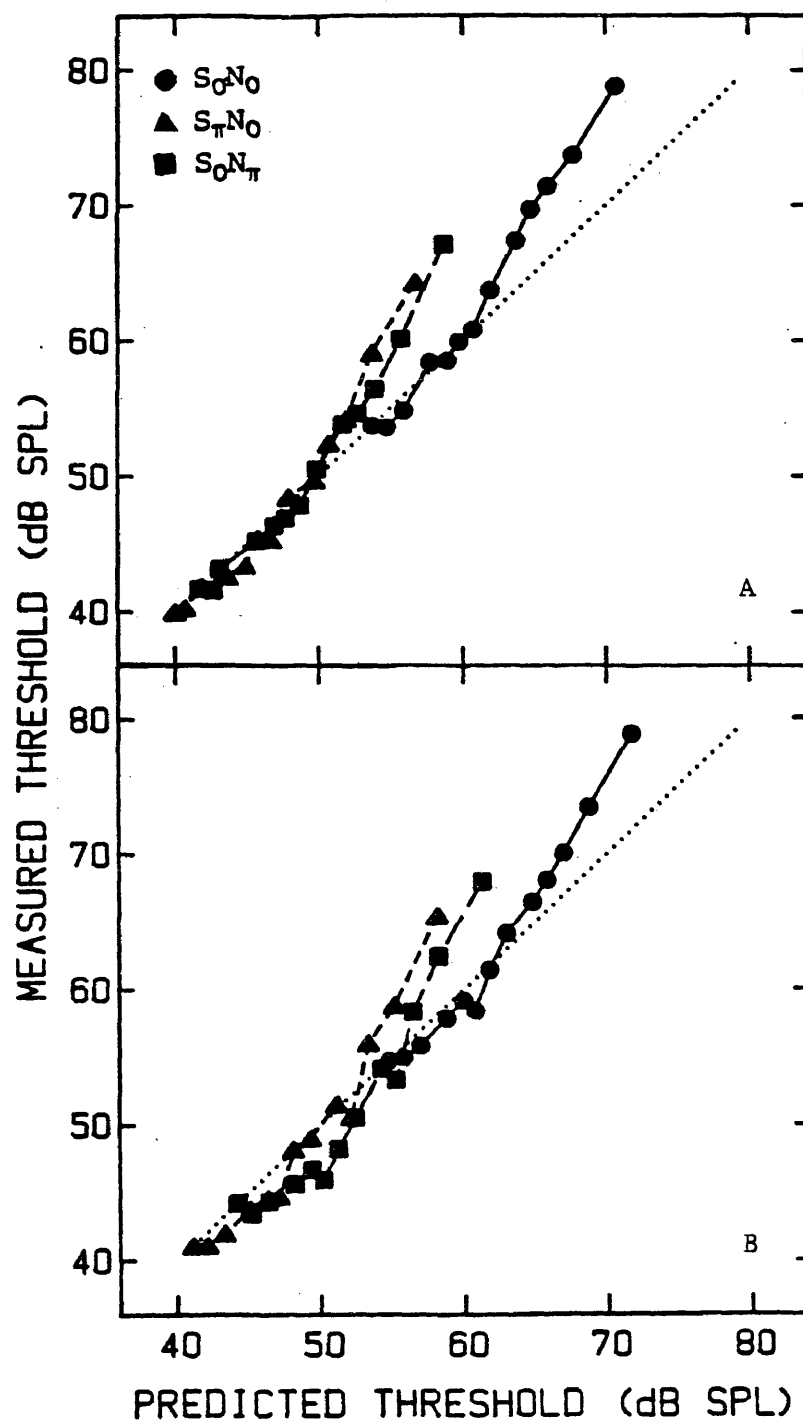


Figure 13. The relation between predicted (abscissa) and measured thresholds (ordinate) in dB SPL for 500-Hz pure tones. The dotted line represents perfect power summation.

level differences that occur as signal duration is varied. In Figure 14 the mean $S_{\pi}N_0$ masking-level differences obtained for the thirteen durations between 2 and 100 ms (triangles) are compared with the masking-level differences reported by Blodgett et al. [(1958), circles]] and Wilson and Fowler [(1985), squares]. Although the masking-level differences for the two subjects in this experiment are slightly larger than those reported by Wilson and Fowler, the general findings are the same. For both studies, the masking-level differences were largest around 8 to 10 ms, and smallest at 2 and 100 ms. The masking-level differences reported by Blodgett et al. reveal the largest masking-level difference at 5 ms, and the smallest at 100 ms. If Blodgett et al. had studied thresholds at signal durations shorter than 5 ms, then a decrease in the masking-level difference at short durations may have been observed. An interesting observation made both in the present study and in the Blodgett et al. study was the occurrence of a "secondary" peak in the masking-level difference functions. This secondary peak occurred at about 30 to 40 ms in the present study, and at 20 ms in the Blodgett et al. study. In addition, the S_0N_{π} masking-level differences observed for both subjects in the present study revealed similar peaks at about 30 ms (see Figure 11). Data from more subjects must be obtained to verify the existence of the secondary peak before explanations for the apparent phenomenon can be attempted. The secondary peaks may represent "noise" in the data or the secondary peaks may reflect an unexplained temporal-related characteristic of the auditory system.

The data displayed in Figures 10, 12, and 13 clearly reveal different breakpoints of the measured threshold functions from the

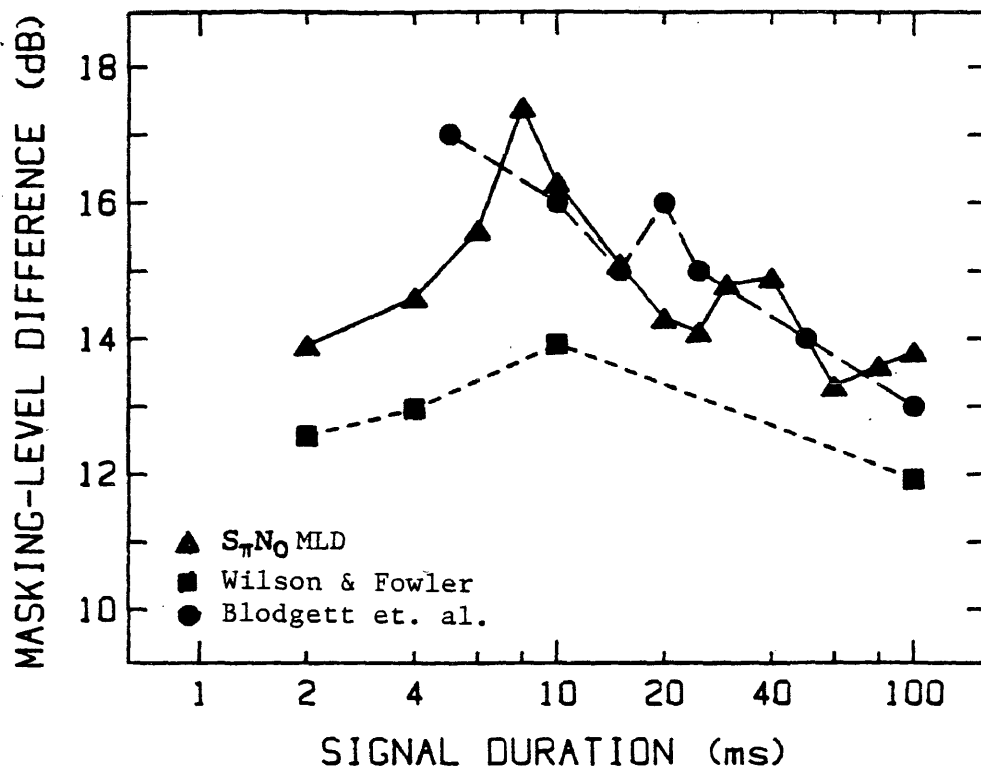


Figure 14. A comparison of the 500-Hz $S_{\pi}N_0$ masking-level differences reported by this study (triangles), Blodgett et. al, [(1958), circles] and Wilson and Fowler [(1985), rectangles].

predicted threshold functions for the S_0N_0 , $S_\pi N_0$, and S_0N_π conditions. One can interpret the breakpoints as indicative of the critical bandwidth. Only energy within the critical bandwidth contributes to the threshold for a signal (Fletcher, 1940). As the duration of a signal is decreased, the signal bandwidth increases (see Table 1). As long as the energy in the bandwidth of the signal is within the critical bandwidth, thresholds continue to increase as predicted by perfect power summation. Once the signal bandwidth exceeds the critical bandwidth, then more energy is required to maintain thresholds than is predicted by perfect power summation. Because the spectral characteristics of the S_0N_0 , $S_\pi N_0$, and S_0N_π signals are identical, the changes in thresholds greater than the changes in threshold predicted by perfect power summation may be attributed to different critical bandwidths for S_0N_0 , $S_\pi N_0$, and S_0N_π . The different breakpoints demonstrated by both subjects for the S_0N_0 and $S_\pi N_0$ functions indicate that the critical bandwidths of various binaural phase conditions are different. Additionally, although the breakpoints in the $S_\pi N_0$ and S_0N_π functions were different for Subject A, Subject B demonstrated identical breakpoints for the respective conditions. The $S_\pi N_0$ and S_0N_π data indicate that while there are differences across subjects, for some subjects, different critical bands may exist for the two conditions.

Table 6 presents estimates of the critical bandwidths for S_0N_0 , $S_\pi N_0$, and S_0N_π , based upon the different breakpoints observed for Subject A and Subject B, respectively. For each condition, the lower and upper limits of the critical bandwidth were calculated using: $[1000 \text{ (ms)}/\text{signal duration (ms)}]$. The duration at which the measured

Table 6. Estimates of the critical bandwidth (in Hz) for S_0N_0 , $S_\pi N_0$, and S_0N_π for Subject A and Subject B.

Condition	Signal Duration (ms) at which		Estimated Critical Bandwidth (Hz)
	M = P (a)	M > P (b)	
Subject 1			
S_0N_0	20	15	50-67
$S_\pi N_0$	10	8	100-125
S_0N_π	15	10	67-100
Subject 2			
S_0N_0	15	10	67-100
$S_\pi N_0$	8	6	125-167
S_0N_π	8	6	125-167

a The measured threshold is equal to the threshold predicted by perfect power summation.

b The measured threshold is higher than the threshold predicted by perfect power summation.

threshold equals the predicted threshold ($M = P$, column 2) is the signal duration from which the lower limit of the critical bandwidth was calculated, whereas the duration at which the measured threshold is higher than the predicted threshold ($M > P$, column 3) is the signal duration from which the upper limit was calculated. The estimated critical bandwidths in Hertz for the three binaural conditions are listed in column 4. In general, the estimated critical bands in Table 6 indicate that the $S_{\pi}N_0$ critical band is wider than the S_0N_0 critical band. The data for Subject A indicate that the S_0N_{π} critical band is wider than the S_0N_0 critical band, but narrower than the $S_{\pi}N_0$ critical band. The data for Subject B, in contrast, reveal no difference in critical bandwidth between $S_{\pi}N_0$ and S_0N_{π} . Sever and Small (1979) estimated the critical bandwidths for S_0N_0 and $S_{\pi}N_0$ for five subjects. The mean critical bandwidths (and ranges) for S_0N_0 and $S_{\pi}N_0$ reported by Sever and Small, 53 Hz (28 to 84 Hz) and 86 Hz (50 to 140 Hz), respectively, are in relatively good agreement with the critical bandwidths estimated in Table 6, thereby supporting the hypothesis that the $S_{\pi}N_0$ critical band is wider than the S_0N_0 critical band.

To summarize, the current data indicate that the effects of reducing signal duration are different for the S_0N_0 and $S_{\pi}N_0$ conditions. These differences were reflected in both the temporal integration functions and the masking-level differences obtained for the 13 signal durations. The estimated critical bandwidths for S_0N_0 and $S_{\pi}N_0$ were also different, suggesting that the underlying auditory processes involved in S_0N_0 and $S_{\pi}N_0$ listening conditions are different.

REFERENCES

- American National Standards Institute. (1969). "Specifications for audiometers, ANSI S3.6-1969." (American National Standards Institute, New York).
- von Békésy, G. (1960). "Neural inhibitory units of the eye and skin. Quantitative description of contrast phenomena." Journal of the Optical Society of America. 50, 1060-1070.
- Blodgett, H. C., Jeffress, L. A., & Taylor, R. W. (1958). "Relation of masked threshold to signal duration for various interaural phase combinations." American Journal of Psychology. 71, 283-290.
- van den Brink, G. (1964). "Experiment on cochlear summation." Journal of the Acoustic Society of America. 36, 1213-1214 (L). (Cited by Scharf, 1970.)
- Elliott, L. L. (1965). "Changes in the simultaneous masked threshold of brief tones." Journal of the Acoustical Society of America. 38, 738-746.
- Feldtkeller, R. & Oettinger, R. (1956). Die Hörbarkeitsgrenzen von Impulsen verschiedener Dauer." Acustica. 6, 489-493. (Cited by Scharf, 1970.)
- Fletcher, H. (1940). "Auditory patterns." Review of Modern Physiology. 12, 47-65.
- Garner, W. R. (1947). "The effect of frequency spectrum on temporal integration of energy in the ear." Journal of the Acoustical Society of America. 19, 808-815.
- Garner, W. R., & Miller, G. A. (1947). "The masked threshold of pure tones as a function of duration." Journal of Experimental Psychology. 37, 293-303.
- Gassler, V. G. (1953). "Over the threshold of audibility for sound stimuli with different widths of the frequency spectrum." Acustica. 4, 408-414.
- Green, D. M. (1966). "Interaural phase effects in the masking of signals of different durations." Journal of the Acoustical Society of America. 39, 720-724.
- Hamilton, P. M. (1957). "Noise masked thresholds as a function of tonal duration and masking noise band width." Journal of the Acoustical Society of America. 29, 506-511.
- Miller, G. A. (1948). "The perception of short bursts of noise." Journal of the Acoustical Society of America. 20, 160-170. (Cited by Scharf, 1970.)

- Levitt, H. (1971). "Transformed up-down methods in psychoacoustics." Journal of the Acoustical Society of America 49, 467-476.
- Miskolczy-Fodor, F. (1959). "Relation between loudness and duration of tonal pulses. I. Response of normal ears to pure tones longer than click-pitch threshold." Journal of the Acoustical Society of America. 31, 1128-1134. (Cited by Scharf, 1970.)
- Plomp, R., & Bouman, M. A. (1959). "Relation between hearing threshold and duration for tone pulses." Journal of the Acoustical Society of America. 31, 749-758.
- Scharf, B. (1970). "Critical Bands." In J. V. Tobias (Ed.), Foundations of Modern Auditory Theory, (Vol. 1, pp. 159-202). New York: Academic.
- Scholl, H. (1962a). "Über die Bildung der Hörschwellen und Mithörschwellen von Impulsen." Acustica. 12, 91-101. (Cited by Scharf, 1970.)
- Scholl, H. (1962b). "Das dynamische Verhalten des Gehörs bei der Unterteilung des Schallspektrums in Frequenzgruppen." Acustica. 12, 101-107. (Cited by Scharf, 1970.)
- Sever, J. C., Jr. & Small, A. M., Jr. (1979). "Binaural Critical Bands." Journal of the Acoustical Society of America. 66 (5), 1343-1349.
- Swets, J. A., Green, D. M., Tanner, W. P., Jr. (1962). "On the width of critical bands." Journal of the Acoustical Society of America. 34, 108-113. (Cited by Scharf, 1970.)
- Wilson, R. H. & Fowler, C. G. (1985). "Effects of signal duration on the 500-Hz masking-level difference." Manuscript submitted for publication.
- Yost, W. A. & Dolan, D. (1978). "Masking-level differences for repeated filtered transients." Journal of the Acoustical Society of America. 63, 1927-1930.
- Yost, W. A. & Silva, D. (1977). "Binaural processing of filtered transients." Sensory Processes. 1, 363-375.
- Zwicker, E. & Wright, H. N. (1963). "Temporal summation for tones in narrow-band noise." Journal of the Acoustical Society of America. 35, 691-699. (Cited by Scharf, 1970.)
- Zwislocki, J. (1961). "Theory of temporal auditory summation." Journal of the Acoustical Society of America. 32 (8), 1046-1060.
- Zwislocki, J. (1965). "Analysis of some auditory characteristics." In R. D. Luce, R. R. Bush, and E. Galanter (Eds.) Handbook of Mathematical Psychology. (Vol. 3, pp. 1-97). New York, NY: Wiley. (Cited by Scharf, 1970.)